Cellulose Nanocrystal–Reinforced Polyvinyl Acetate Nanolatex for Viscose Fabric Prepregs and Composite Materials

Journal of Applied Polymer Science

WILEY

Applied Polymer SCIENCE

RESEARCH ARTICLE OPEN ACCESS

Cellulose Nanocrystal–Reinforced Polyvinyl Acetate Nanolatex for Viscose Fabric Prepregs and Composite Materials

Shahab Nasr[1] | Pooria Khalili[1] | Gunnar Westman[2] | Mikael Skrifvars[1]

[1]Swedish Centre for Resource Recovery, University of Borås, Borås, Sweden | [2]Chalmers University of Technology, Gothenburg, Sweden

Correspondence: Shahab Nasr (shahab.nasr@hb.se)

Received: 16 June 2025 | **Revised:** 31 October 2025 | **Accepted:** 6 November 2025

Keywords: mechanical properties | packaging | synthesis and processing techniques

ABSTRACT

In this study, polyvinyl acetate (PVAc)-based nanocomposite latexes containing varying loads of cellulose nanocrystals (CNCs), a sodium salt of sulfated nanocrystalline cellulose, were synthesized and utilized as a matrix for fabricating fiber-reinforced composites with viscose fabric. A CNC-free PVAc matrix was used as the reference. The composites were fabricated via compression molding of hand-layup-prepared prepregs. The objective of this study was to assess the applicability of CNC-modified latexes as a matrix and evaluate the effect of CNC loading on composite performance and properties. CNC incorporation was characterized by FTIR to identify the hydroxyl groups and their potential interactions with the matrix and fabric. Mechanical testing was performed via tensile, impact, flexural, and interlaminar shear strength (ILSS) measurements. Although CNC addition reduced the elastic modulus, all samples demonstrated higher elongation at break, with a maximum increase of 31%. The 1.2 wt% CNC-loaded composite exhibited the most promising performance, showing a 13.7% increase in ultimate tensile strength, a 36.2% increase in impact resistance, and an improvement of 56% and 46% in flexural strength and ILSS, respectively. Microscopic analyses revealed that CNC incorporation enhanced the structural integrity of the composite layers. These findings highlight the potential of CNC-reinforced PVAc latexes in the development of sustainable composite materials.

1 | Introduction

Polyvinyl acetate and viscose textile fabrics can be combined to form composites with improved properties, making them suitable for diverse applications such as fusible interlining for clothing or care products [1–3]. The application of PVAc–viscose composites in structural or semi-structural products, such as packaging, represents the potential utilization of these materials. The hydrophilic similarity between polyvinyl acetate latex (matrix) and cellulosic fillers (viscose) enhances the properties and fabrication of composites by providing more available bonding sites. Mechanical properties of composites can be affected by the selection of short or continuous natural fibers [4], while the advantage of continuous fibers or woven fabrics over short fibers has been reported in the literature [5]. Parameters such as fiber arrangement, bulkiness and porosity are different for woven from nonwoven fibers [6]. Among the different natural fibers, regenerated cellulose fibers, such as viscose, are distinctive as they are produced in a synthetic process from natural cellulose sources. Considering composites with high fracture toughness, viscose fibers have shown reliable results [7]. The synthetic man-made viscoses provide uniformity in mechanical, size, and physical properties. Moreover, parameters such as biodegradability, carbon dioxide neutrality, and low density are related to their natural origins [8]. Uniformity of regenerated cellulose fibers, along with useful parameters in manufacturing composites, were our derivatives to select them in this study. However, the application

of polyvinyl acetate latex as a matrix has certain limitations. For instance, polyvinyl acetate latex after drying cannot stand against water adsorption [9].

Sodium sulfated cellulose nanocrystals (CNCs), as renewable and bio-based reinforcements, offer potential improvements in the performance of water-based polymer matrices [10–12]. The incorporation of CNC into polyvinyl acetate (PVAc) latex may enhance properties such as water resistance and mechanical strength. Additionally, potential interactions between the CNC-containing latex and viscose fabric can contribute to the functional characteristics relevant to the fabrication of composites. In this context, the incorporation of polyvinyl alcohol in the synthesis of polyvinyl acetate could bring some advantages enhancing composite manufacturing [13]. The application of vinyl acetate monomers produced via bioethanol in synthesizing polyvinyl acetate makes them closer to a biobased product [14, 15]. Polymerization of vinyl acetate is conventionally carried out through water-based emulsion polymerization [16, 17]. Lower process temperature, lower volatile organic compound content, and safer processing conditions make them suitable alternatives to solvent-based polymers. In our previous study, we demonstrated the successful synthesis of nanocomposite-modified latex from vinyl acetate monomers and cellulose nanocrystals via emulsion polymerization. The synthesized nanocomposite latexes exhibited a high solid content, which is consistent with the findings of Nozaki and Lona [18]. It has been reported that the mechanical properties of CNC and polyvinyl alcohol composites are influenced by their interaction, especially through the control of processing parameters [19]. In another study by Chatterjee, Singh and Chaudhary [20], nonwoven viscose fabric and polyvinyl alcohol were used to fabricate a biodegradable composite. The results showed proper connection between polyvinyl alcohol (PVA) and viscose fibers through FESEM and FTIR results.

This study presents a novel approach to fabricate composites using cellulose nanocrystal (CNC) modified polyvinyl acetate latex in combination with viscose fabrics. Although the modification of latex with CNCs has been previously reported [18, 21], this work is the first to employ such modified latex as a matrix in the fabrication of fiber-reinforced composites from viscose fabrics using a prepreg method. The process was conducted under mild conditions, both in the water-based synthesis of the CNC-PVAc matrix and during composite fabrication, which was carried out under low pressure and temperature. This provides a low-energy, scalable, and environmentally friendly alternative to conventional composite manufacturing methods. The prepreg technique facilitates uniform resin distribution, simplifies the production process, and mitigates common challenges such as poor wetting and nanoparticle aggregation during fabrication.

The resulting composites were evaluated through a comprehensive set of mechanical tests including tensile, flexural, impact, and interlaminar bending tests. The incorporation of CNCs significantly improved the interfacial adhesion between the latex matrix and viscose fibers, leading to enhanced mechanical performance and structural integrity. The use of CNC in latex not only contributes to improved composite properties, but also supports the development of bio-based, process-efficient materials for potential use in packaging and related applications. To the best of our knowledge, this is the first study to integrate CNC-modified latex with viscose fabric in a prepreg process, establishing a new pathway for producing high-performance, sustainable composites.

In our study, polyvinyl acetate latex modified with cellulose nanocrystals was used as the composite matrix, whereas pristine polyvinyl acetate latex served as the reference. The addition of CNCs is expected to influence the final properties of the composites. Woven viscose fabrics were selected as reinforcement and converted into prepreg materials through matrix impregnation. This approach allowed for water removal from latex, facilitating pre-composite processing in a manner compatible with industrial requirements. The prepregs were subsequently molded at 60°C to produce 0°/90° biaxial multilayer composite laminates. All composites were fabricated with approximately 34–39 wt% fiber content in a 0°/90° orientation lay-up procedure. The mechanical properties, including the tensile, impact, interlaminar, and flexural properties, were evaluated according to established standards. In addition, a water absorption test was conducted to assess the resistance of the composites to moisture uptake. Microscopic analysis was conducted to identify defects in the samples following the impact tests, and the matrix was examined separately to detect any processing-related issues.

2 | Materials and Methods

2.1 | Materials

The viscose was a warp-knitted uniaxial fabric supplied by ENGTEX with an areal density of 223 g^{-2}. The matrix was polyvinyl acetate latex with incorporated cellulose nanocrystals, and a pristine polyvinyl acetate homopolymer latex was used as a reference. Vinyl acetate (≥ 99%, Sigma Aldrich) was used as received without further purification. Ammonium peroxydisulfate $(NH_4)_2S_2O_8$ (Alfa Aesar, Kandel, Germany), and sodium bicarbonate (Sigma Aldrich) were used as received. Partially saponified polyvinyl alcohol (PVA 8–88) was sourced from Kuraray Europe GmbH, Germany. Commercial CNCs featuring sulfate half-ester surface groups with Na^+ as a counterion were procured from CelluForce Inc. (Montreal, Québec, Canada). Distilled water was prepared using Milli-Q (IQ 7000, 18.2 mΩ.cm@25°C). Matrix synthesis was performed through in situ emulsion polymerization. In short, to prepare 1 kg of the nanocomposite latex, sodium sulfated cellulose nanocrystals were dispersed in approximately 400 g of deionized water by magnetic stirring followed by 15 min of sonication. Approximately 10 wt% of a prepared polyvinyl alcohol (PVA) solution was then added to the CNC suspension. This CNC solution was then added to the reactor and heated to 70°C. The reaction started with the addition of 41.3 wt% of ammonium persulfate solution and 3 wt% of vinyl acetate. After 15 min, the remaining monomer, initiator, and protective colloid solutions were continuously added through separate inlets to the reactor for approximately 5 h. Nanocomposite latex with different loadings of CNCs was synthesized according to this procedure and was used for composite production. Pristine homopolymer latex (H/V) was synthesized without CNC as a reference. Table 1 presents the CNC loadings of all matrix formulations.

2.2 | Composite Manufacturing Using Prepregs

Composite laminates were manufactured from prepregs composed of six viscose fabrics placed on top of each other in a 0°/90° alternating orientation. Table 2 provides the composition of the composites, with the weight percentages of the viscose and latex matrix.

To manufacture the prepregs, the viscose fabric was cut into 20 × 20 cm pieces, and six fabrics were placed in a 0°/90° arrangement in successive layers. The viscose fabric stacks were then dried overnight in an oven at 60°C prior to the manufacture of the prepregs. To prepare the prepregs, a 1000 μm thick wet film of latex was made with a film applicator on Teflon paper, and the precut dried viscose stack was immediately placed on it. Latex impregnation was performed manually using a hand lay-up method, ensuring thorough saturation of the fabrics. The prepregs were then stored overnight under ambient laboratory conditions and dried in an oven for 24 h at 45°C. The prepregs were stored in sealed plastic bags before composite production.

The prepregs were first preheated at 60°C for 10 min, and then compression molded using a hot pressing machine at 60 kN (0.95 MPa) and 60°C for 12 min. Teflon paper was used to isolate the prepregs from the hot-press surfaces. After pressing, the composite laminate was removed and placed on a flat surface under a weight of approximately 1.5 kg (233 Pa) until it cooled and was ready for characterization. All specimens for the mechanical tests were prepared using a laser-cutting machine to ensure precise geometry and consistent dimensions. The laser parameters were optimized to minimize the localized heating and prevent thermal degradation or edge defects. No visual signs of burning or delamination were observed along the edges of the specimens after cutting. Figure 1 illustrates the schematic of the composite fabrication process.

2.3 | Tensile Test

Tensile testing was performed in accordance with the EN ISO 527-4 2023 (Type 1 specimen) standard using a Tinius Olsen H10KT testing machine (Horsham, PE, USA) equipped with a 100 R mechanical extensometer connected to the middle of the samples possessing the initial distance between grips of 115 mm for strain measurement. For each sample, eight dumbbell-shaped specimens were tested along the fiber machine direction at a speed of 2 mm/min. All the samples were

TABLE 1 | Composition of nanocomposites (NC) and pristine homopolymer latex.

Samples (Matrices)	Vinyl acetate [g]	Water [g]	Ammonium persulfate [g]	Sodium bicarbonate [g]	Polyvinyl alcohol 8–88 [g]	Wt% of CNC based on weight of vinyl acetate in nanocomposite	Total solid content (TSC) %
Nanocomposite 1 (NC1)	465	498.2	0.78	0.74	12.78	0.6	49–51
Nanocomposite 2 (NC2)	465	498.2	0.78	0.74	12.78	1.2	49–51
Nanocomposite 3 (NC3)	465	498.2	0.78	0.74	12.78	1.9	49–51
Nanocomposite 4 (NC4)	465	498.2	0.78	0.74	12.78	2.5	49–51
Nanocomposite 5 (NC5)	465	498.2	0.78	0.74	12.78	3.2	49–51
Poly (vinyl acetate) (H)	465	498.2	0.78	0.74	12.78	—	49–51

TABLE 2 | Composition of fiber and matrix in composite samples.

Samples	Total weight of six prepregs [g]		Total weight of six viscose sheet [g]	Total weight of matrix for six sheets [g]	Wt% of viscose	Wt% of matrix
	Before drying	After drying				
Composite 1 (NC1/V)	180.2	171.6	65.4	106.2	38	62
Composite 2 (NC2/V)	172.3	163.9	64.2	99.7	39	61
Composite 3 (NC3/V)	176.7	170.7	64.2	106.5	37	63
Composite 4 (NC4/V)	197.8	190.2	65.4	124.8	34	66
Composite 5 (NC5/V)	181.1	175.2	65.6	109.6	37	63
Composite 6 (H/V)	191.6	182.7	65.3	117.4	35	65

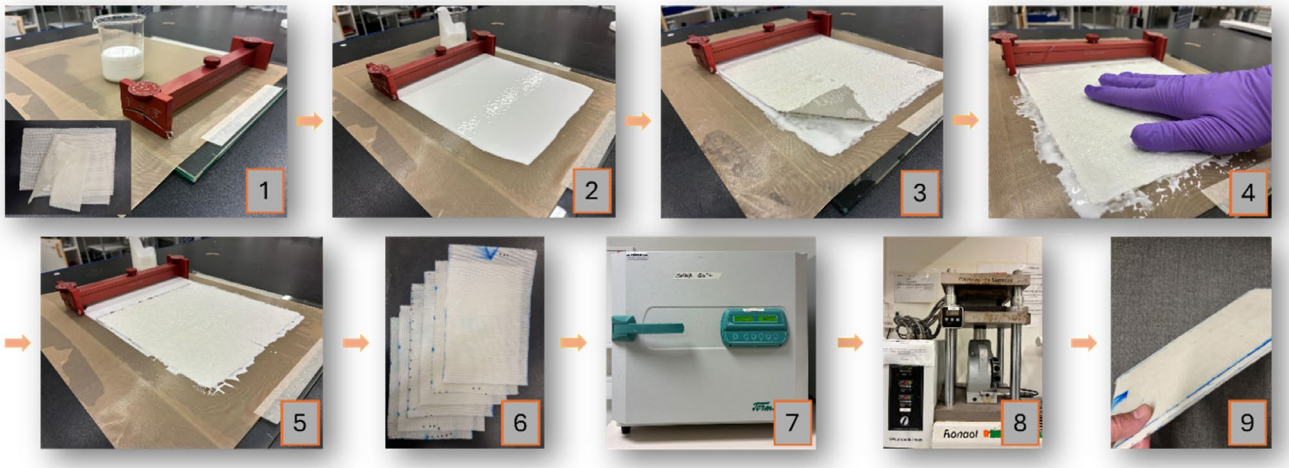

FIGURE 1 | Photographic illustration of the composite fabrication (1) Adjustment of the film applicator to 1000 μm; preparation of nanocomposites or homopolymer latex and viscose sheets (2) Casting a wet film on a Teflon paper (3) Placing the viscose sheet onto the wet film (4) Hand lay-up to form the prepregs (5) Drying the prepregs under laboratory conditions (6) Prepregs after overnight drying at the laboratory conditions (7) Additional drying of the prepregs in an oven at 45°C for 24 h (8) Hot pressing of the dried prepregs (9) Final fabricated composite. [Color figure can be viewed at wileyonlinelibrary.com]

conditioned in a climate chamber for 48 h at 23°C and 50% relative humidity before testing. The initial gauge length was 50 mm, gripping pressure was 4.5 bar and extensometer and crosshead speed were 2 mm/min. The samples were clamped using pneumatic grips at a pressure of 4.5 bar, ensuring adequate holding without slippage or cracking in accordance with EN ISO 527-1. The standard deviations and mean values were calculated.

2.4 | Charpy Impact Test

Charpy impact testing was conducted following the BS EN ISO 179-1 standards using a Cometech QC-639D testing instrument (Taichung, Taiwan). The pendulum hammer weighed 3.409 kg and had an impact length (L_i) of 395 mm (mass center distance of 354 mm) and an energy capacity of 22 J. Five un-notched specimens from each composite sample were tested flatwise and edgewise, as specified by the standard, to determine the average impact strength. The results were expressed in kilojoules per square meter (kJ/m^2). The specimen width was 10 mm, and the length was 80 mm according to the specimen type 1, and the span was 62 mm. The influence of bearing friction and air resistance on the energy loss was considered negligible for all samples. All the samples were placed in a climate chamber for 48 h at 23°C and 50% relative humidity before testing.

2.5 | Interlaminar Shear Test of Composites

The interlaminar shear strength (ILSS) was evaluated using a specialized ILSS test fixture in accordance with the ASTM D2344 standard. The tests were conducted using a Tinius Olsen H10KT testing machine (Horsham, PE, USA). Five specimens of each sample were tested at a speed of 1 mm/min. The specimens were prepared according to the standard, with dimensions where the length was six times the thickness and the width twice the thickness. The span between the supports was 16 mm, and the beam was loaded in three-point bending. The samples were maintained in a climate chamber for 48 h at 23°C and 50% humidity before testing. The Short-Beam Strength was calculated using Equation (1):

Short-Beam Strength:

$$E_f = 0.75\,\frac{P_m}{bh} \tag{1}$$

where P_m is the maximum force and b and h are the width and thickness of the samples, respectively.

2.6 | Flexural Test of Composites

The flexural properties were determined by three-point bending according to the BS EN ISO 14125 standard on a Tinius Olsen H10KT testing machine (Horsham, PE, USA). To ensure consistency and accuracy, all the specimens were conditioned for 48 h at 23°C and 50% humidity prior to testing. The testing protocol used a crosshead speed of 1 mm/min, with a support span of 40 mm. Testing was conducted with a 5 kN load cell, and each sample measured 60 mm in length and 15 mm in width (Method A, Class III). To reach the confidence interval, the average values and standard deviations were calculated for all the composites based on five identical specimens. The flexural modulus of elasticity was calculated based on Equation (2):

Flexural Modulus:

$$E_f = \frac{L^3}{4bh^3}\left(\frac{\Delta F}{\Delta S}\right) \tag{2}$$

where E_f is flexural modulus of elasticity expressed in MPa, L is the support span (mm), b indicates the beam's width (mm), h is the beam's thickness (mm), and $\Delta F/\Delta S$ is the slope of the initial linear segment of the load versus deflection curve (N/mm), corresponding to deflection.

2.7 | Fourier Transform Infrared Spectroscopy (FTIR)

The approximate peak intensities of the hydroxyl groups in the nanocomposite matrices were examined using an ATR-FTIR spectrophotometer (Nicolet iS10, Thermo Scientific, Waltham, MA, USA). For quantitative characterization, spectra were recorded in the absorbance mode across the 400–4000 cm^{-1} wavenumber range, with a resolution of 4 cm^{-1} and 64 accumulated scans per spectrum.

2.8 | Water Absorption

Water absorption was determined for all samples in accordance with EN ISO 62:2008 [22]. The samples were dried at 45°C in an oven for 72 h and allowed to cool to room temperature in a desiccator prior to the test. Three replicates were used for each composite. The samples were soaked in containers filled with distilled water under laboratory conditions (23°C). The amount of water absorption was measured as the weight gain percentage for all samples. M_o is the mass of the sample after the initial drying and before immersion, and M is the weight after water absorption. The average mass gain of the three test samples for each composite was calculated and reported as an increasing percentage of the weight gain. The mass gain (W) is the percentage change in mass relative to the initial mass and is calculated using Equation (3):

$$W = \frac{M - M_0}{M_0} \times 100 \quad (3)$$

2.9 | Polarization Optical Microscopy

An optical polarized light microscope (Nikon LV100ND) equipped with a Nikon DS-Fi3 camera was used to examine the cracks or delamination areas of the nanocomposite matrix and composites after the impact tests. Image acquisition and analysis were conducted using NIS-Elements software (version 5.41.01). The collected images were used to analyze the nanocomposite latex and post-tested composite samples.

2.10 | Data Analysis

Statistical analysis of the experimental data was conducted using Minitab 21.1.1 (2022 Minitab LLC, USA). One-way ANOVA was used to evaluate statistical differences among the samples. Levene's test indicated that the assumption of homogeneity of variance was met (P-value > 0.05). Group comparisons were performed using paired t-tests, with the significance level set at 0.05.

3 | Results and Discussion

3.1 | Tensile Properties of Composites

The tensile yield strength, ultimate strength, E Modulus, and elongation at break of all the composites are shown in Figure 2.

The yield strengths of all composites with the CNC-modified matrix were lower than that of the H/V reference composite. According to Figure 2a, the NC4/V composite exhibited the highest reduction, reaching 7.7 MPa (37.3% lower than H/V composite). Statistical comparison of the samples to the H/V composite showed that the yield strengths of NC1/V, NC4/V, and NC5/V decreased significantly (P-value < 0.05), while the NC2/V and NC3/V composites showed no significant decrease. The lowest reduction, only 1.3 MPa lower (6.3% lower) than the H/V composite, was measured for the NC2/V composite (P-value = 0.153). The results showed that the incorporation of CNC within the matrix caused lower resistance to withstand the applied stress and a lower deformation possibility within the elastic region compared to the H/V composite. It might correspond to the poor interfacial bonds between nanocellulose and polymer chains which prohibit the elastic change of the composite [23, 24]. Therefore, all NC/V composites withstand lower stresses before starting plastic deformation compared to the H/V composite. As is illustrated in Figure 2b, the ultimate strength of composites increased significantly (P-value = 0.002) for NC2/V composite with 55.6 MPa which was 13.7% higher than reference H/V composite with 48.9 MPa. The ultimate strength of the NC1/V composite with the lowest CNC loading remained unchanged. According to these results, increasing the CNC loading to a value higher than that used in CN2/V caused a reduction in the ultimate strength, as shown in Figure 2b. The reduction trend started from the NC3/V composite and reached a minimum of 35.9 MPa for the NC5/V composite, which was 26.6% lower than that of the H/V composite. Although the statistical analysis showed that significant reduction to the H/V reference composite was only for NC4/v and NC5/V.

Figure 2c shows the modulus of elasticity of the composites. The elastic modulus of composites depends on the properties of both the matrix and fabric. In our study, both macro- and nanofillers were incorporated into the manufacturing of composites, which imparted specific properties to the final composite. The composition of the composites was almost the same for the volume fraction of the macro filler (viscose) and orientation of the filler, and all composites were tested under the same conditions of temperature and humidity. The results showed the same trend as previously discussed for yield stress. However, except for NC3/V (P-value = 0.109), all composites exhibited a significantly lower E-modulus (P-value < 0.05) than the H/V composite.

Figure 2d also illustrates the variation in the elongation at break among the composite samples. The participation of CNC within the matrix for all samples showed higher elongation, which almost gradually increased up to NC5, 31.5% higher than that of the H/V composite. Similar results of plastic deformation were previously reported by Gong, Mathew and Oksman for nanocomposites of CNC and poly (vinyl acetate) [25]. There was an exception to the increasing trend in elongation at break for the

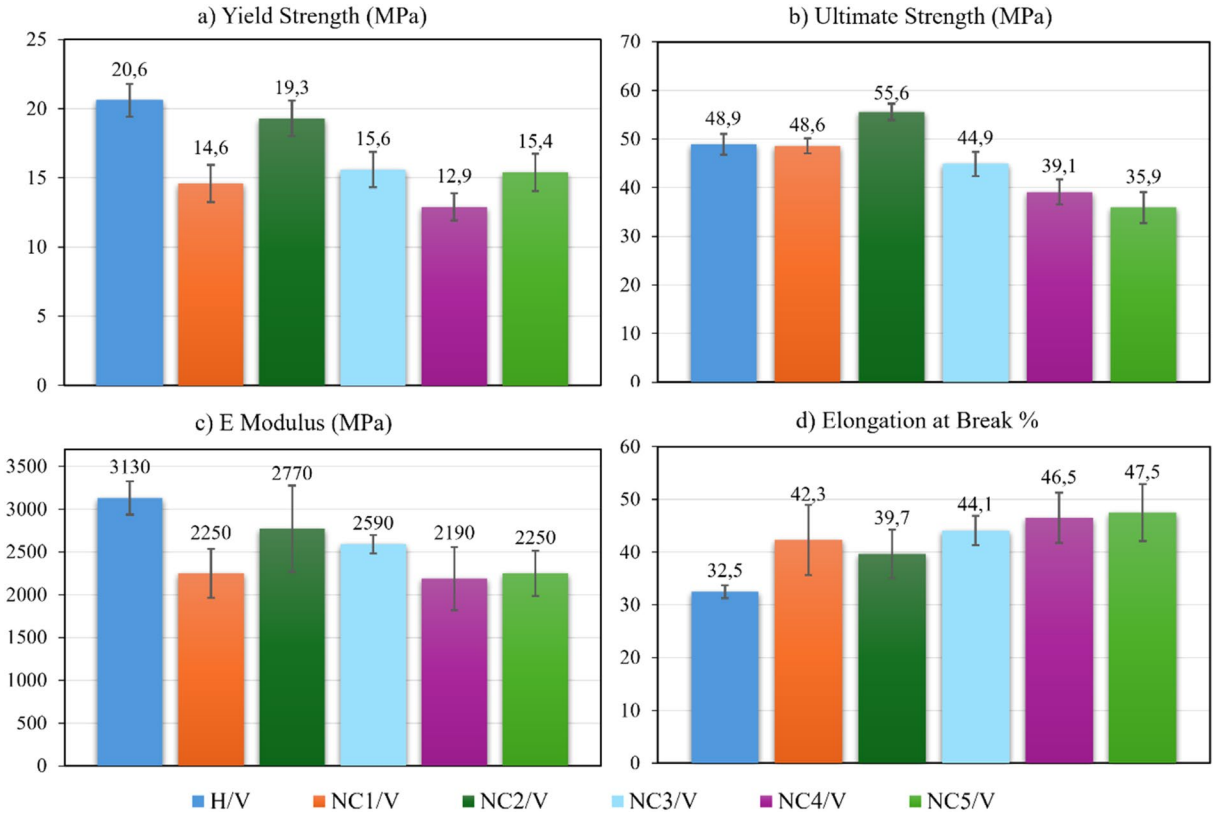

FIGURE 2 | Tensile properties for CNC-PVAc-viscose composites. (a) Yield strength, (b) Ultimate strength, (c) *E* Modulus, and (d) Elongation at break for all composites (Error bars represent standard deviations). [Color figure can be viewed at wileyonlinelibrary.com]

NC2/V composites. The increasing trend was not consistent for the NC2/V composite; however, the NC2/V composite exhibited an 18.1% higher elongation at break than the H/V composite, while remaining 6.1% lower than the NC1/V composite. The reason for the lower elongation at break for NC2/V is not entirely clear, although it could be attributed to variations in the processing conditions, either in the manufacturing of the matrix or in the fabrication of the composite. The results show that the incorporation of CNC in the fabrication of nanocomposites significantly improves the stretching of the samples before breakage (*P*-value for all NC/V composites was lower than 0.05). Therefore, the nanocomposite matrix helps to achieve greater ductility and the ability to undergo elongation at break of the composites, making them suitable for applications requiring flexibility and toughness.

As illustrated in Figure 3, all composites exhibited a lower modulus of elasticity than the H/V reference. It might be related to the disruption of the polymer network caused by the addition of CNC [23]. CNCs might introduce interactions that enhance flexibility rather than stiffness, which makes the composites more compliant, as shown by the higher elongation at break (Figure 2d). Incorporation of CNCs can indeed lead to alterations in polymer chain mobility. In our study, the effect of CNC in elastic regions promoted higher compliance, which caused lower stiffness. The flexibility (elongation at break) of the nanocomposite/viscose composites might be under the influence of hydrogen bonding between CNC and polymer chains [26].

During the tensile test, delamination into separate layers was observed in the H/V and NC5/V composite samples, whereas no delamination occurred in the other samples. This suggests that a proper interfacial bond was formed between the matrix and the viscose fabric in the NC1/V to NC4/V composites, maintaining the structural integrity prior to reaching the maximum CNC loading in NC5/V. The tensile tests also revealed differences in fracture location. While approximately 50% of H/V samples fractured at the center (gauge section), the NC/V composites exhibited a higher frequency of breakage at the neck. Fractures at the neck or near the grips may be attributed to stress concentration or uneven stress distribution, potentially caused by variations in processing conditions.

3.2 | Charpy Impact Damage Behavior

The Charpy impact strength is shown in Figure 4. The results indicated that incorporating CNCs of up to 1.9 wt% of vinyl acetate monomer in the manufacturing of the matrix positively influences the impact strength for NC1/V to NC3/V. However, the effect of CNC was only statistically significant for NC2/V and NC3/V (*P*-value < 0.05). This effect diminishes as the CNC content increases to 2.5 and 3.2 wt% for NC4/V and NC5/V, respectively. Geng, Haque [21] reported similar toughness results due to the increment of CNC in the manufacturing of in situ nanocomposite of CNC and polyvinyl acetate. As illustrated in Figure 5, CNCs improved the toughness until NC3/V, which might be related to the efficient distribution and connections of

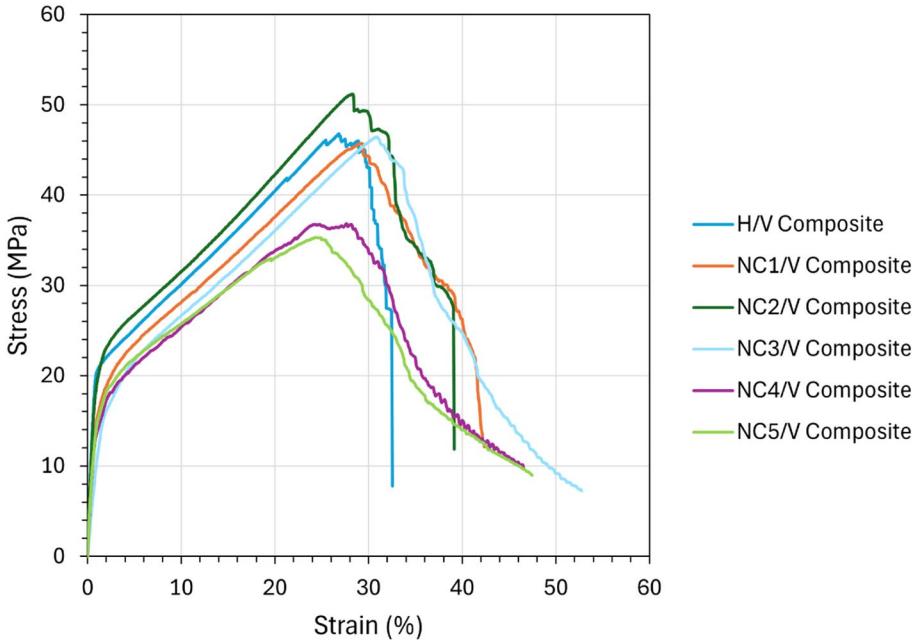

FIGURE 3 | Stress–Strain curves under tensile test for all composites. [Color figure can be viewed at wileyonlinelibrary.com]

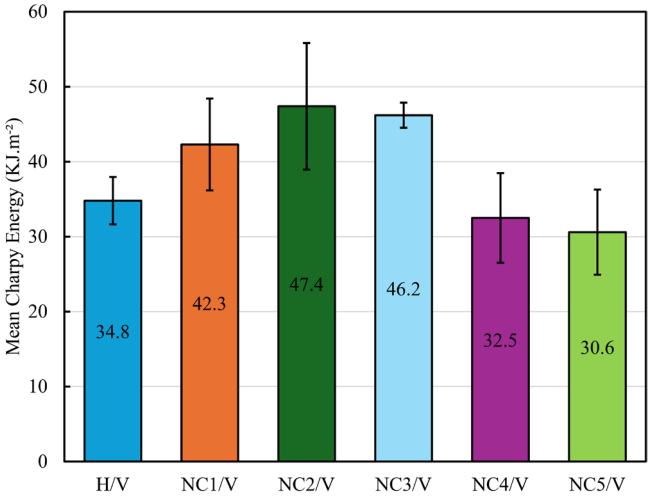

FIGURE 4 | The result of Charpy impact test for all composites (Error bars represent standard deviations). [Color figure can be viewed at wileyonlinelibrary.com]

CNC and polymer chains. A higher loading of CNC might deteriorate the uniform dispersion of CNC in the polymer matrix (latex), which prohibits the appropriate filler/matrix interface.

The improved impact strength was also reflected in the stability and integrity of the composites. Visual images taken from the post-impact tests are shown in Figure 5. Only NC2/V and NC3/V exhibited the highest impact strength and retained their structural integrity without exhibiting significant or complete delamination. However, the microscopic images of these samples revealed microscale delamination at the fracture points (Figure 10). In contrast, the homopolymer and other nanocomposite latexes used as matrices failed to prevent layer delamination after the impact. Interactions between CNC and polyvinyl alcohol have been previously reported, highlighting the plasticizing effect of polyvinyl alcohol. The disruption of hydrogen bonding within the CNC network has been identified as a key factor leading to a reduction in elastic modulus and an increase in the toughness of bacterial nanocellulose–PVA nanocomposites [23]. These findings are supported by our experimental results, which also demonstrate the influence of varying the CNC loading on the mechanical properties. While a lower loading of CNCs for NC1/V improved the impact strength, it did not influence the integrity of the composite layers after the test. The effect of CNC showed a higher impact and integrity of the composite for NC2/V and NC3/V when the CNCs were loaded moderately (Table 1). However, this effect was diminished by increasing CNC loading to a greater extent than that of NC3/V. For NC4/V and NC5/V, the impact strength decreased, but not significantly (*P*-value higher than 0.05), to a lesser extent than that of the H/V composite. It might be related to the areas where CNCs accumulate or agglomerate in a way that there was not proper connection available between nanofillers, polymers and viscose.

3.3 | Interlaminar Shear Test of Composites

The interlaminar shear tests are illustrated in Table 3 based on the results obtained for vinyl acetate latex composites reinforced with woven viscose fiber, focusing on the impact of incorporating cellulose nanocrystals (CNC) within latex at varying concentrations. The results are discussed based on the vinyl acetate viscose (H/V) composite as a baseline exhibiting the short-beam strength of 2.6 MPa and a maximum force of 104 N. Initially, the incorporation of CNC into the vinyl acetate latex improved the short-beam strength and maximum force of the composites at the two lowest concentrations (NC1/V and NC2/V). This increment reached the highest performance for NC2/V (1.2 wt% CNC; Table 1) with the short-beam strength of 3.8 MPa (46% more than baseline) and a maximum force of 148 N, suggesting effective performance at this loading. This improvement can be attributed to the potential of the CNC to strengthen the matrix, which consequently improves the overall composite strength.

The relationship between CNC loading and interlaminar shear strength is clearly nonlinear. Initially, increasing the CNC content improved performance, suggesting an effective reinforcement mechanism. However, beyond a certain threshold, further increases in CNC loading led to a decrease in performance, indicating potential drawbacks such as agglomeration and processing challenges. The extracted stress–strain data are shown in Figure 6 to illustrate the effect of CNC on the composite samples. Here, the maximum short-beam shear stress was observed for NC2/V, while the lowest value was for NC4/V. NC2/V exhibited the highest ILSS, which is consistent with its curve reaching the highest value between the samples before failure. This indicates an effective stress transfer and enhanced interlaminar bonding. The results of the ILSS tests reflected the effectiveness of the load transfer and resistance to shear stress between the layers (matrix and reinforcement) up to the NC2/V composite.

According to Sapkota, Kumar, Weder and Foster [27], CNCs may contribute to stiffer and stronger vinyl acetate matrices, thereby allowing for a more efficient load distribution. Additionally, the high aspect ratio and surface area of CNCs could promote a more robust fiber-matrix interphase, facilitating improved

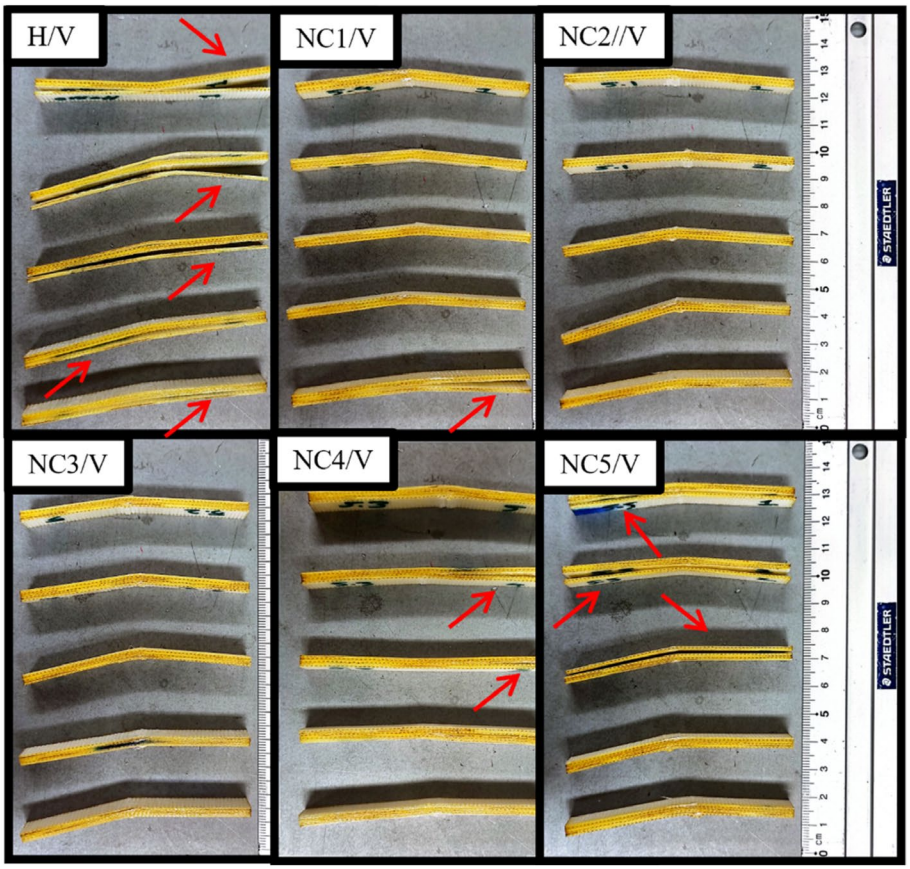

FIGURE 5 | Composite samples after Charpy Impact tests; delaminated points are pointed out with arrows. [Color figure can be viewed at wileyonlinelibrary.com]

TABLE 3 | Inter-laminar shear test of composites.

Samples	Maximum force [N]	Standard deviation of maximum force [N]	Width [mm]	Thickness [mm]	(ILSS) Short-beam strength [MPa]
H/V composite	104	26.4	8	3.7	2.6
NC1/V composite	125	60.3	8	3.7	3.1
NC2/V composite	148	39.4	7.9	3.6	3.8
NC3/V composite	122	9.74	7.9	3.6	3
NC4/V composite	110.6	31	7.9	4	2.5
NC5/V composite	131	1.92	7.9	3.8	3.2

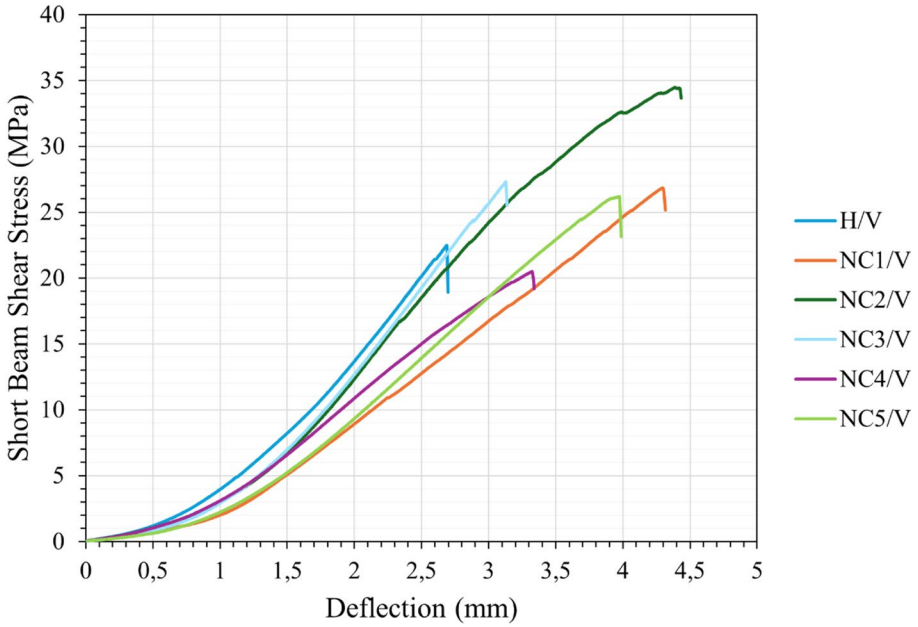

FIGURE 6 | Short-beam shear stress–deflection diagram of the composite samples. [Color figure can be viewed at wileyonlinelibrary.com]

stress transfer from the matrix to the reinforcing viscose fibers [28]. Furthermore, the presence of CNCs in the latex may affect the interlaminar region via interlaminar bonding by providing higher resistance against shear forces [29]. However, exceeding the optimal loading of CNC beyond NC2/V resulted in a decline in performance. From NC3/V to NC5/V, both the short-beam strength and maximum force started to decrease, exhibiting a maximum reduction in the short-beam strength for NC4/V, which was even lower than the H/V baseline. While NC3/V exhibited a slight decrease compared to NC2/V, NC4/V exhibited the lowest performance among the CNC-modified composites. The reduction in performance at higher CNC concentrations suggests potential drawbacks associated with excessive CNC loading [30].

One possible explanation for this is the agglomeration of CNC within the latex matrix. The uniform dispersion of CNCs becomes more challenging at higher concentrations, resulting in agglomerates or microscale CNC domains. These agglomerates could disrupt the matrix continuity and create weak points [31]. Moreover, the higher viscosity of the modified latex as a consequence of higher CNC loading, potentially hinders the proper wetting of the viscose fibers during prepreg preparation [32]. Inadequate fiber wetting can lead to an increased void content and a weaker matrix–fiber interphase. It is also possible that CNCs may induce embrittlement of the matrix or even interfere with the in situ polymerization process [33].

3.4 | Flexural Properties of Composites

Figure 7 illustrates the flexural modulus and flexural strength (including the standard deviations) of the composites. The homopolymer viscose composite (H/V) exhibited a flexural modulus of 2147 MPa, which was selected as the baseline. As shown in Figure 7, the modification of the matrix with different CNC loadings resulted in a nonlinear response for the composites. While the incorporation of CNC at the two lowest loadings (NC1/V and NC2/V; Table 1) led to a significant reduction (P-values < 0.05) in the flexural modulus (Figure 8a), an increase in CNC content resulted in enhanced stiffness for NC3/V and NC4/V, which was not significantly different (P-value > 0.05) compared to the H/V composite baseline (Figure 8a). Regarding the NC5/V composite, the reduction in flexural modulus was not significant compared with the baseline (P-value $= 0.074$). The flexural strength showed a different trend, indicating almost no effect on NC1/V (Figure 8b). A significant increase in flexural strength was observed for NC2/V (P-value $= 0.025$), with a mean value of 50 MPa. NC3/V and NC5/V showed improved strength compared with the H/V baseline, which was not statistically significant (P-value > 0.05). NC4/V exhibited a significant reduction (P-value $= 0.039$) in flexural strength among all the samples.

The most significant enhancement in flexural strength was observed at 1.2 wt% CNC loading (NC2/V; Table 1), with an increase to mean value of 50 MPa compared to H/V baseline of 32 MPa. The 57% improvement in flexural strength at NC2/V suggests that CNCs effectively enhance the load-bearing capacity at this specific concentration of CNC for the modification of the matrix. Mechanical properties of nanocomposite materials are directly related to microstructure parameters such as proper dispersion and interfacial bonding between matrix and filler [34]. The flexural strength results aligned with general understanding of nanofiller reinforcement in composites and conducted studies for optimal incorporation of CNC [34–36]. Fine particles tend to combine together and form tightly bound aggregates, which can further develop into larger agglomerated structures [36]. The non-linear trend of flexural strength demonstrated a significant reduction in NC4/V at 18 MPa. A possible explanation for this reduction could be CNC agglomeration leading to stress concentrations or processing deficiencies related to increased viscosity of matrix (due to the higher CNC concentration; Table 1) hindering viscose fiber wetting [32]. The agglomeration of CNCs may be attributed to insufficient chemical bonding with polymer chains, leading to poor dispersion of

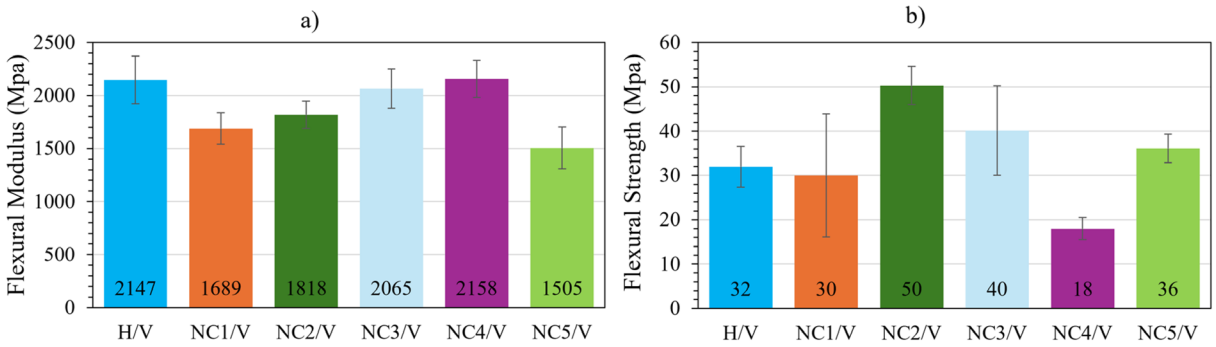

FIGURE 7 | Flexural properties of vinyl acetate/viscose composites with varying CNC loadings: (a) Flexural Modulus (MPa), (b) Flexural Strength (MPa). (Error bars represent standard deviations). [Color figure can be viewed at wileyonlinelibrary.com]

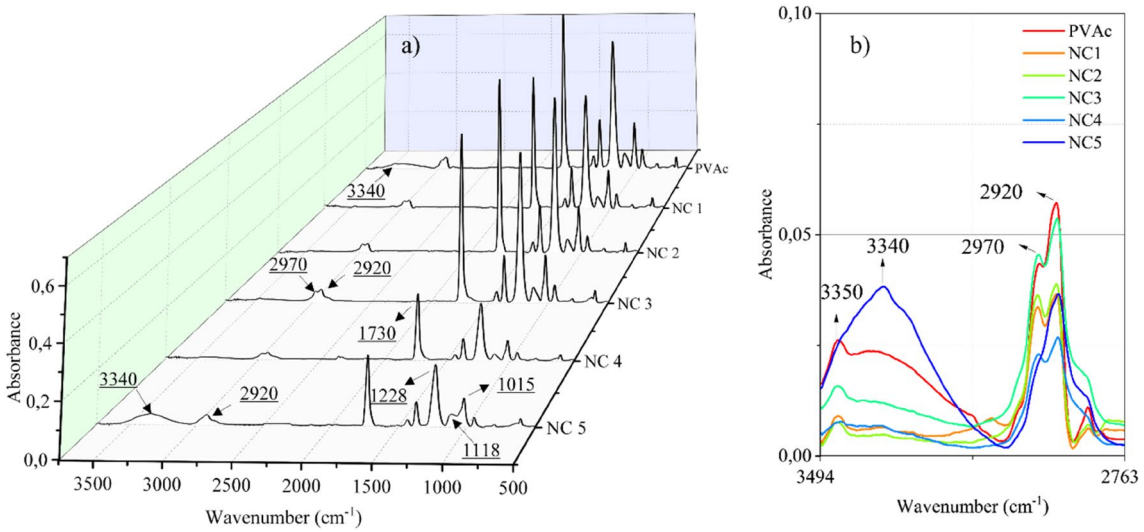

FIGURE 8 | (a) FTIR spectra for poly (vinyl acetate) and nanocomposite latex, (b) Enlarged scale of OH group for all samples. [Color figure can be viewed at wileyonlinelibrary.com]

the nanofiller and consequently limiting the reinforcement efficiency and effective load transfer. Moreover, there is a volume fraction limit for incorporation of nanoparticles into the polymer matrix [36]. The effect of a higher volume fraction of CNC on the stiffness of composites was previously observed in the results of the tensile test (Figure 2). Previous experimental investigation on nanocomposite materials indicated a same results for reduction in bending strength after critical nanofiller volume fraction [37]. Agglomeration, especially for large aggregations, could affect the bending strength more than smaller aggregates [38]. Considering NC5/V, a significantly higher flexural strength was observed compared to NC4/V (P-value = 0.004), but there was no statistically significant difference from the H/V composite baseline. The FTIR results for NC5 (modified matrix; Table 1) showed higher available hydroxyl groups, which could be considered as a reason for the formation of a kind of network between the CNCs. It is assumed that at higher CNC loadings, an interconnected network of CNCs may form, potentially enhancing the load transfer efficiency within the composite. Further investigation is required to confirm this assumption. The observations of the flexural modulus of the composites compared to the H/V baseline suggested that CNCs may not effectively contribute to increasing the resistance to deformation (stiffness) of the composite system. As shown in Figure 8a, incorporating CNC into composites led to a decrease in stiffness, initially causing a sharp reduction in NC1/V, followed by a gradual improvement up to NC4/V. Although the reduction in stiffness was significant for NC1/V and NC2/V (P-value < 0.05), it had no significant effect on the other composites.

3.5 | Fourier-Transform Infra-Red Spectroscopy

FTIR spectroscopy was employed to detect specific chemical interactions between the functional groups following the incorporation of CNCs into poly (vinyl acetate) latex. Figure 8a presents the FTIR spectra of the pristine PVAc homopolymer and its nanocomposites with various CNC loadings.

The broad absorption band between 3200 and 3500 cm^{-1} is attributed to O–H stretching vibrations, indicative of intra- and intermolecular hydrogen bonding. The most prominent peak was observed at 3340 cm^{-1} for NC5, followed by PVAc at 3350 cm^{-1}. This band exhibited a noticeable decrease in intensity compared to the other nanocomposite samples (Figure 8b). For the highest CNC loading in NC5, the increased intensity of this peak may indicate the presence of free cellulose nanocrystals dispersed within the aqueous phase. The presence of free CNCs may also contribute to the agglomeration and formation of stress concentration zones within the final dried nanocomposite.

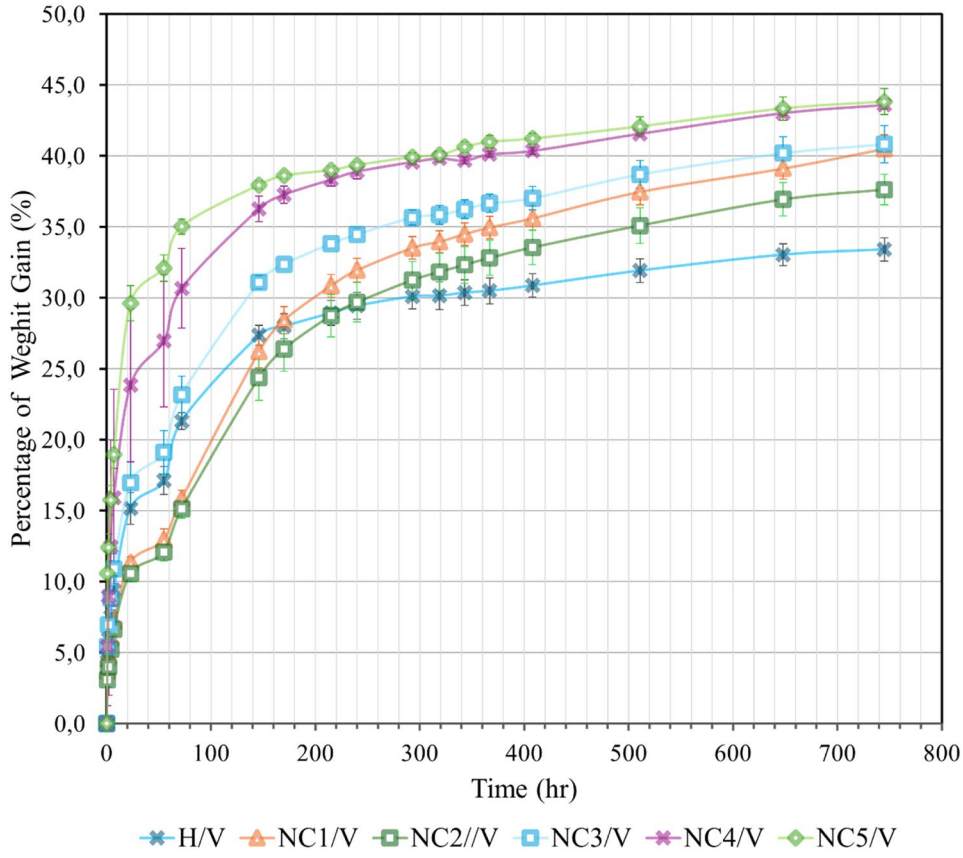

FIGURE 9 | The percentage of weight gain of composites after immersion in water. [Color figure can be viewed at wileyonlinelibrary.com]

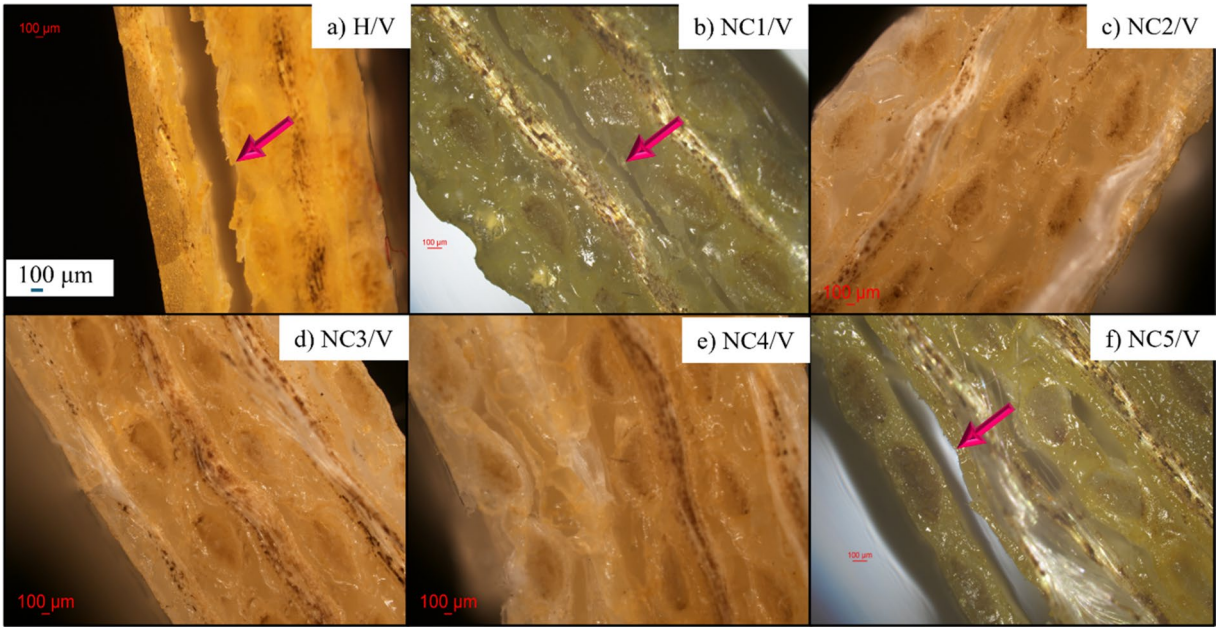

FIGURE 10 | Microscopic images of composite samples after impact, (a) H/V (matric cracking and delamination), (b) NC1/V (matrix cracking; without detectable delamination), (c) NC2/V (matrix cracking, delamination at micro scale), (d) NC3/V (matrix cracking, delamination at micro scale), (e) NC4/V (matrix cracking, delamination at micro scale), (f) NC5/V (matrix cracking and delamination). [Color figure can be viewed at wileyonlinelibrary.com]

It is a common interaction in polymer blends for hydrogen bonding to occur between hydroxyl groups (as in CNC) and carbonyl groups (as in polyvinyl acetate) [39]. However, the reduction in the intensity of the ester carbonyl (C═O) bands in NC4 and NC5 may be attributed to the higher CNC content relative to PVAc in these samples, as the frequencies remained unchanged. If the carbonyl groups are involved in hydrogen bonding with CNC, a shift to lower frequencies is expected.

3.6 | Water Absorption of Composites

Figure 9 illustrates the percentage of mass gain for the fabricated composites over the immersion time (in hours) at 23°C. During the first 24 h, the water absorption values of the NC1/V and NC2/V composites were the lowest at 11.3% and 10.5%, respectively. The H/V composite was the third lowest during the initial 24 h of water absorption (15.1%), whereas NC3/V, NC4/V, and NC5/V exhibited water absorption rates of 16.9%, 23.8%, and 29.6%, respectively. Subsequently, the water absorption rate increased slightly for all the samples, maintaining a consistent trend up to 60 h. During this period, the smallest increase was observed for NC2/V at 1.5%, whereas the largest increase was recorded for NC5/V at 10.7%. From 60 to 160 h, all the composites experienced the second sharpest increase in water absorption. The highest increase was recorded for NC1/V (17.1%), followed by NC2/V (15.9%). After 160 h and up to 1 month, the water absorption rate decreased for all samples. H/V, NC4/V, and NC5/V showed the lowest increments, while NC1/V and NC2/V exhibited the highest. The saturation of all composites was not fully achieved even after 1 month of immersion, indicating the strong resistance of the bonds between the matrix and viscose to prolonged water exposure. No signs of disintegration were observed for the composites throughout the test.

The results indicated that CNC incorporation into latex influenced the water absorption to 1.2 wt% of CNC (Table 1). By increasing the CNC content higher than 1.2 wt% (Table 1) in the manufacturing of the nanocomposites matrix, water absorption by the composite was promoted compared to the H/V reference. It could be attributed to the hydrophilic nature of the CNCs due to the hydroxy groups available on the surface which was promoted by increasing the unconnected CNCs within the matrix [40]. Since the filler content (viscose) was constant across all composites, the variation in water adsorption was primarily influenced by the CNC loading. According to Angkuratipakorn, Singkhonrat [40], CNCs absorb water more readily than conventional cellulose, particularly through the C2-OH and C3-OH groups. For NC1/V and NC2/V, CNCs might be connected by interfacial bonds between polymer chains, which causes a reduction of possible sites (hydroxy groups) for water absorption. The water absorption of NC1/V reached the level of the reference composite (H/V) approximately 170 h after immersion, whereas NC2/V required 220 h to reach the same level. The comparison of CNC content in NC2 and NC1 (Table 1) indicated that a higher CNC concentration did not lead to increased water absorption. This suggests improved dispersion and interactions between polyvinyl acetate and CNC during the modification of the matrix up to a certain amount of CNC. To evaluate the effect of water absorption, the dried films of the reference matrix and five CNC-modified matrices were subjected to water absorption testing. For the reference matrix, that is, pristine poly (vinyl acetate), one-hour immersion in water resulted in visible disintegration, while, except for the NC5 matrix, other CNC-modified matrices remained stable. The results of this study showed that all the composites remained structurally stable after the test. The bonding sites created between the matrix and viscose influenced the stability of the composite, leading to an overall reduction in hydrophilicity.

3.7 | Polarized Optical Microscopy

The post-impact samples were examined using a polarized optical microscope to assess structural defects, such as matrix cracking, fiber breakage, or delamination. These observations are presented in Figure 10. The H/V samples consistently exhibited complete delamination with clearly defined layer separation. The incorporation of CNC into the latex matrix resulted in a considerable improvement in the post-impact structural integrity; however, this effect diminished when the CNC loading exceeded an optimal threshold, resulting in behavior similar to the H/V reference.

As shown in Figure 10, the NC1/V samples remained largely intact in 80% of the cases, although microcracks were detected within the matrix without any evident delamination at the matrix–fiber interface. In NC2/V and NC3/V, all specimens retained structural integrity, although small microcracks were observed. Upon reaching a CNC content of 2.5 wt% (NC4/V), partial delamination was detected in approximately 60% of the samples, accompanied by larger cracks. Complete delamination with extensive cracking was observed in all NC5/V samples.

These results indicate that moderate CNC loading enhances matrix cohesion and promotes improved interfacial bonding between the matrix and viscose fiber. In contrast, excessive CNC content likely leads to stress concentration points that initiate crack formation. Additionally, microscopic investigation was

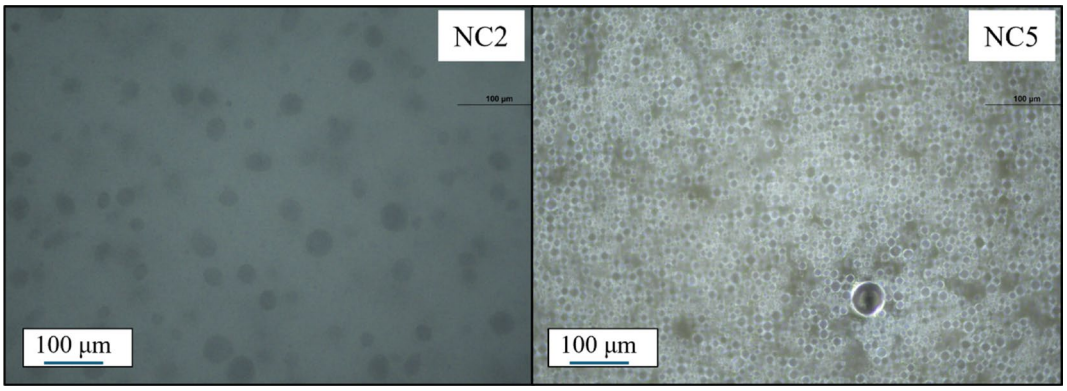

FIGURE 11 | Microscopic images of air bobbles in nanocomposite latex, left (NC2) and right (NC5). [Color figure can be viewed at wileyonlinelibrary.com]

performed on the applied matrices. Microscopic analysis of the wet nanocomposite matrices revealed the presence of numerous air bubbles, the density of which increased with higher CNC loadings (Figure 11). These entrapped air bubbles may have contributed to the crack propagation during mechanical testing. It is also possible that air bubbles were entrapped between the prepregs during composite fabrication, which could adversely affect the final quality and structural integrity of the composites.

4 | Conclusions

The results of this study demonstrated the effect of CNC loading on both the matrix properties and composite performance. CNC incorporation enhanced several properties up to an optimal concentration, beyond which a decline in performance was observed. The modified matrices exhibited improved structural stability and lower delamination at appropriate loadings.

The mechanical properties of composites are influenced by the concentration of CNCs in the matrix. Composites prepared with CNC-modified matrices exhibited higher elongation at break and flexural strength, indicating improved ductility and resistance to bending stress. The results of tensile and flexural tests showed that CNCs had a limited effect on the stiffness of the fabricated composites. The results of the interlaminar shear strength (ILSS) aligned with the results of the flexural test of the effectiveness of CNC at moderate concentrations. A similar trend was observed in Charpy impact tests.

These findings highlight the potential of CNC as bio-based nanofillers to optimize the matrix performance and enhance composite integrity. Overall, this study underscores the importance of adjusting the CNC content to balance the stiffness and flexibility for specific applications.

Author Contributions

Shahab Nasr: conceptualization (lead), data curation (lead), formal analysis (lead), investigation (lead), methodology (lead), software (lead), validation (lead), visualization (lead), writing – original draft (lead), writing – review and editing (equal). **Pooria Khalili:** conceptualization (supporting), data curation (supporting), formal analysis (supporting), investigation (supporting), methodology (lead), supervision (supporting), validation (supporting), writing – review and editing (equal). **Gunnar Westman:** conceptualization (supporting), data curation (supporting), resources (supporting), supervision (supporting), writing – review and editing (supporting). **Mikael Skrifvars:** conceptualization (supporting), funding acquisition (supporting), investigation (supporting), methodology (supporting), project administration (lead), resources (supporting), supervision (lead), writing – review and editing (supporting).

Acknowledgments

The authors thank our lab technicians Ville Skrifvars, Magnus Götlind, and Jonas Hansson for their technical support in performing the experiments.

Funding

The authors have nothing to report.

Ethics Statement

The authors have nothing to report.

Conflicts of Interest

The authors declare no conflicts of interest.

Data Availability Statement

The data are available from the corresponding author upon reasonable request.

References

1. S. M. Mortazavi and P. E. Boukany, "Application of Mixtures of Resin Finishing to Achieve Some Physical Properties on Interlining Cotton Fabrics: I-Effect of Stiffening and Cross-Linking Agents," *Iranian Polymer Journal (English Edition)* 13, no. 3 (2004): 213–218+249.

2. W. Roggenstein, "Viscose Fibers With New Functional Characteristics," *Technische Textilien* 53, no. 4 (2010): 134–136.

3. U. Vrabič and D. Gregor-Svetec, "Properties of Regular Viscose Fibres Used in Feminine Care Products," *Tekstilec* 47, no. 9–12 (2004): 305–307.

4. O. Faruk, A. K. Bledzki, H.-P. Fink, and M. Sain, "Biocomposites Reinforced With Natural Fibers: 2000–2010," *Progress in Polymer Science* 37, no. 11 (2012): 1552–1596, https://doi.org/10.1016/j.progpolymsci.2012.04.003.

5. D. Scida, A. Bourmaud, and C. Baley, "Influence of the Scattering of Flax Fibres Properties on Flax/Epoxy Woven Ply Stiffness," *Materials & Design* 122 (2017): 136–145, https://doi.org/10.1016/j.matdes.2017.02.094.

6. D. Das, A. K. Pradhan, R. Chattopadhyay, and S. Singh, "Composite Nonwovens," *Textile Progress* 44, no. 1 (2012): 1–84, https://doi.org/10.1080/00405167.2012.670014.

7. R. B. Adusumali, M. Reifferscheid, H. Weber, T. Roeder, H. Sixta, and W. Gindl, "Mechanical Properties of Regenerated Cellulose Fibres for Composites," in *Macromolecular Symposia*, vol. 244 (Wiley Online Library, 2006), 119–125.

8. S. K. Ramamoorthy, F. Bakare, R. Herrmann, and M. Skrifvars, "Performance of Biocomposites From Surface Modified Regenerated Cellulose Fibers and Lactic Acid Thermoset Bioresin," *Cellulose* 22 (2015): 2507–2528, https://doi.org/10.1007/s10570-015-0643-x.

9. L. Xinghai, Y. Shengping, H. Chi, and L. Houbing, "Preparation of Poly (Vinyl Acetate) Modified by Triethoxyvinylsilane and Properties of Copolymeric Lattices," *Iranian Polymer Journal* 16, no. 3 (2007): 207–213.

10. A. S. Pakdel, V. Gabriel, R. M. Berry, C. Fraschini, E. D. Cranston, and M. A. Dubé, "A Sequential Design Approach for In Situ Incorporation of Cellulose Nanocrystals in Emulsion-Based Pressure Sensitive Adhesives," *Cellulose* 27, no. 18 (2020): 10837–10853, https://doi.org/10.1007/s10570-020-03060-6.

11. A. S. Pakdel, E. Niinivaara, E. D. Cranston, R. M. Berry, and M. A. Dubé, "Cellulose Nanocrystal (CNC)–Latex Nanocomposites: Effect of CNC Hydrophilicity and Charge on Rheological, Mechanical, and Adhesive Properties," *Macromolecular Rapid Communications* 42, no. 3 (2021): 2000448, https://doi.org/10.1002/marc.202000448.

12. Y. Wang, B. Sun, Z. Hao, and J. Zhang, "Advances in Organic–Inorganic Hybrid Latex Particles via In Situ Emulsion Polymerization," *Polymers* 15, no. 14 (2023): 2995, https://doi.org/10.3390/polym15142995.

13. N. Jelinska, M. Kalnins, A. Kovalovs, and A. Chate, "Design of the Elastic Modulus of Nanoparticles-Containing PVA/PVAc Films by the Response Surface Method," *Mechanics of Composite Materials* 51 (2015): 669–676, https://doi.org/10.1007/s11029-015-9537-0.

14. B. Rieger, A. Künkel, G. W. Coates, R. Reichardt, E. Dinjus, and T. A. Zevaco, *Synthetic Biodegradable Polymers*, vol. 245 (Springer Science & Business Media, 2012).

15. S. Carrà, A. Sliepcevich, A. Canevarolo, and S. Carrà, "Grafting and Adsorption of Poly (Vinyl) Alcohol in Vinyl Acetate Emulsion Polymerization," *Polymer* 46, no. 4 (2005): 1379–1384, https://doi.org/10.1016/j.polymer.2004.11.061.

16. J. M. Asua, *Polymeric Dispersions: Principles and Applications*, vol. 335 (Springer Science & Business Media, 2012).

17. Y. H. Erbil, *Vinyl Acetate Emulsion Polymerization and Copolymerization With Acrylic Monomers* (CRC Press, 2000).

18. A. P. Nozaki and L. M. Lona, "Comparison Between Cellulose Nanocrystal and Microfibrillated Cellulose as Reinforcement of Poly (Vinyl Acetate) Composites Obtained by Either In Situ Emulsion Polymerization or a Simple Mixing Technique," *Cellulose* 28 (2021): 2273–2286, https://doi.org/10.1007/s10570-021-03691-3.

19. E. Niinivaara, J. Desmaisons, A. Dufresne, J. Bras, and E. D. Cranston, "Thick Polyvinyl Alcohol Films Reinforced With Cellulose Nanocrystals for Coating Applications," *ACS Applied Nano Materials* 4, no. 8 (2021): 8015–8025, https://doi.org/10.1021/acsanm.1c01244.

20. A. Chatterjee, H. Singh, and K. Chaudhary, "Nonwoven Viscose Fabric-Polyvinyl Alcohol Based Flexible Composite," *Journal of Vinyl and Additive Technology* 29, no. 1 (2023): 41–47, https://doi.org/10.1002/vnl.21941.

21. S. Geng, M. M.-U. Haque, and K. Oksman, "Crosslinked Poly (Vinyl Acetate) (PVAc) Reinforced With Cellulose Nanocrystals (CNC): Structure and Mechanical Properties," *Composites Science and Technology* 126 (2016): 35–42, https://doi.org/10.1016/j.compscitech.2016.02.013.

22. ISO, *Plastics—Determination of Water Absorption*, vol. BS EN ISO 62:2008 (International Organization for Standardization, 2008).

23. D. Ray and S. Sain, "In Situ Processing of Cellulose Nanocomposites," *Composites Part A: Applied Science and Manufacturing* 83 (2016): 19–37, https://doi.org/10.1016/j.compositesa.2015.09.007.

24. M. Ghasemlou, F. Daver, E. P. Ivanova, Y. Habibi, and B. Adhikari, "Surface Modifications of Nanocellulose: From Synthesis to High-Performance Nanocomposites," *Progress in Polymer Science* 119 (2021): 101418, https://doi.org/10.1016/j.progpolymsci.2021.101418.

25. G. Gong, A. P. Mathew, and K. Oksman, "Toughening Effect of Cellulose Nanowhiskers on Polyvinyl Acetate: Fracture Toughness and Viscoelastic Analysis," *Polymer Composites* 32, no. 10 (2011): 1492–1498, https://doi.org/10.1002/pc.21170.

26. H. D. Huang, C. Y. Liu, L. Q. Zhang, G. J. Zhong, and Z. M. Li, "Simultaneous Reinforcement and Toughening of Carbon Nanotube/Cellulose Conductive Nanocomposite Films by Interfacial Hydrogen Bonding," *ACS Sustainable Chemistry and Engineering* 3, no. 2 (2015): 317–324, https://doi.org/10.1021/sc500681v.

27. J. Sapkota, S. Kumar, C. Weder, and E. J. Foster, "Influence of Processing Conditions on Properties of Poly (Vinyl Acetate)/cellulose Nanocrystal Nanocomposites," *Macromolecular Materials and Engineering* 300, no. 5 (2015): 562–571, https://doi.org/10.1002/mame.201400313.

28. H. J. Kim and W. J. Lee, "The Influence of Cellulose Nanocrystal Characteristics on Regenerative Silk Composite Fiber Properties," *Materials* 16, no. 6 (2023): 2323, https://doi.org/10.3390/ma16062323.

29. A. Mohammadpour-Haratbar, S. B. A. Boraei, M. T. Munir, Y. Zare, and K. Y. Rhee, "A Model for Tensile Strength of Cellulose Nanocrystals Polymer Nanocomposites," *Industrial Crops and Products* 213 (2024): 118458, https://doi.org/10.1016/j.indcrop.2024.118458.

30. A. Asadi, M. Miller, R. J. Moon, and K. Kalaitzidou, "Cellulose Nanocrystals as Reinforcement in Glass Fiber/Epoxy Sheet Molding Compound Composites," in *Annual Technical Conference – ANTEC, Conference Proceedings*, (2016).

31. M. L. Shofner, "Processing-Structure-Property Relationships in Cellulose Nanocrystal/Waterborne Epoxy Composites," in *TAPPI International Conference on Nanotechnology for Renewable Materials 2014*, (2014).

32. S. Beck and J. Bouchard, "Ionic Strength Control of Sulfated Cellulose Nanocrystal Suspension Viscosity," *Tappi Journal* 15, no. 6 (2016): 363–372, https://doi.org/10.32964/tj15.6.363.

33. N. Macke, C. M. Hemmingsen, and S. J. Rowan, "The Effect of Polymer Grafting on the Mechanical Properties of PEG-Grafted Cellulose Nanocrystals in Poly(Lactic Acid)," *Journal of Polymer Science* 60, no. 24 (2022): 3318–3330, https://doi.org/10.1002/pol.20220127.

34. G. García del Pino, A. C. Kieling, A. Bezazi, et al., "Hybrid Polyester Composites Reinforced With Curauá Fibres and Nanoclays," *Fibers and Polymers* 21 (2020): 399–406, https://doi.org/10.1007/s12221-020-9506-7.

35. G. da Silva Maradini, M. P. Oliveira, G. M. da Silva Guanaes, et al., "Characterization of Polyester Nanocomposites Reinforced With Conifer Fiber Cellulose Nanocrystals," *Polymers* 12, no. 12 (2020): 2838, https://doi.org/10.3390/polym12122838.

36. M. Šupová, G. S. Martynková, and K. Barabaszová, "Effect of Nanofillers Dispersion in Polymer Matrices: A Review," *Science of Advanced Materials* 3, no. 1 (2011): 1–25, https://doi.org/10.1166/sam.2011.1136.

37. A. L. Gershon, D. P. Cole, A. K. Kota, and H. A. Bruck, "Nanomechanical Characterization of Dispersion and Its Effects in Nano-Enhanced Polymers and Polymer Composites," *Journal of Materials Science* 45 (2010): 6353–6364, https://doi.org/10.1007/s10853-010-4597-y.

38. A. Krishnan and L. R. Xu, "A Simple Effective Flaw Model on Analyzing the Nanofiller Agglomeration Effect of Nanocomposite Materials," *Journal of Nanomaterials* 2012 (2012): 6357–6358, https://doi.org/10.1155/2012/483093.

39. T. Ohno and Y. Nishio, "Miscibility and Intermolecular Interaction of Cellulose Alkyl Ester/Vinyl Polymer Blends," in Polymer Preprints, Japan, (2005).

40. T. Angkuratipakorn, J. Singkhonrat, and A. A. Christy, "Comparison of Water Adsorption Properties of Cellulose and Cellulose Nanocrystals Studied by Near-Infrared Spectroscopy and Gravimetry," *Key Engineering Materials* 735 (2017): 235–239.